Imaging

Cerebrovascular Diseases

Cerebrovasc Dis 2013;36:167–172
DOI: 10.1159/000352048

Received: March 20, 2013
Accepted: May 10, 2013
Published online: October 12, 2013

Progression of Brain Lesions in Relation to Hyperperfusion from Subacute to Chronic Stages after Experimental Subarachnoid Hemorrhage: A Multiparametric MRI Study

Ivo A.C.W. Tiebosch[a] Walter M. van den Bergh[b, c] Mark J.R.J. Bouts[a]
René Zwartbol[a] Annette van der Toorn[a] Rick M. Dijkhuizen[a]

[a]Biomedical MR Imaging and Spectroscopy Group, Image Sciences Institute, and [b]Department of Intensive Care Medicine, University Medical Center Utrecht, Utrecht, and [c]Department of Critical Care, University Medical Center Groningen, Groningen, The Netherlands

Key Words
Animal stroke models · Blood-brain barrier · Cerebral blood flow · Delayed cerebral ischemia · Magnetic resonance imaging · Stroke imaging · Subarachnoid hemorrhage

Abstract
Background: The pathogenesis of delayed cerebral injury after aneurysmal subarachnoid hemorrhage (SAH) is largely unresolved. In particular, the progression and interplay of tissue and perfusion changes, which can significantly affect the outcome, remain unclear. Only a few studies have assessed pathophysiological developments between subacute and chronic time points after SAH, which may be ideally studied with noninvasive methods in standardized animal models. Therefore, our objective was to characterize the pattern and correlation of brain perfusion and lesion status with serial multiparametric magnetic resonance imaging (MRI) from subacute to chronical after experimental SAH in rats. ***Methods:*** SAH was induced by endovascular puncture of the intracranial bifurcation of the right internal carotid artery in adult male Wistar rats (n = 30). Diffusion-, T2-, perfusion- and contrast-enhanced T1-weighted MRI were performed on a 4.7-tesla animal MR system to measure cytotoxic and vasogenic edema, hemodynamic parameters and blood-brain barrier permeability, respectively, at days 2 and 7 after SAH. The neurological status was repeatedly monitored with different behavioral tests between days –1 and 7 after SAH. Lesioned tissue – identified by edema-associated T2 prolongation – and unaffected tissue were outlined on multislice images and further characterized based on tissue and perfusion indices. Correlation analyses were performed to evaluate relationships between different MRI-based parameters and between MRI-based parameters and neurological scores. ***Results:*** Similar to clinical SAH and previous studies in this experimental SAH model, mortality up to day 2 was high (43%). In surviving animals, neurological function was significantly impaired subacutely, and tissue damage (characterized by T2 prolongation and diffusion reduction) and blood-brain barrier leakage (characterized by contrast agent extravasation) were apparent in ipsilateral cortical and subcortical tissue as well as in contralateral cortical tissue. Notably, ipsilateral cortical areas revealed increased cerebral blood flow and volume. Animals that subsequently died between days 2 and 7 after SAH had markedly elevated ipsilateral perfusion levels at day 2. After a week, neurological function had improved in surviving animals, and brain edema

1015–9770/13/0363–0167$38.00/0

E-Mail karger@karger.com
www.karger.com/ced

Rick M. Dijkhuizen
Biomedical MR Imaging and Spectroscopy Group
Image Sciences Institute
Heidelberglaan 100, NL–3584 CX Utrecht (The Netherlands)
E-mail r.m.dijkhuizen@umcutrecht.nl

was partially resolved, while blood-brain barrier permeability and hyperperfusion persisted. The degree of brain damage correlated significantly with the level of perfusion elevation ($r = 0.78$ and 0.85 at days 2 and 7, respectively; $p < 0.05$). Furthermore, chronic (day 7 after SAH) blood-brain barrier permeability and vasogenic edema formation were associated with subacute (day 2 after SAH) hyperperfusion ($r = 0.53$ and 0.66, respectively; $p < 0.05$). ***Conclusion:*** Our imaging findings indicate that SAH-induced brain injury at later stages is associated with progressive changes in tissue perfusion and that chronic hyperperfusion may contribute or point to delayed cerebral damage. Furthermore, multiparametric MRI may significantly aid in diagnosing the brain's status after SAH.

Introduction

Aneurysmal subarachnoid hemorrhage (SAH) is a serious health problem with an incidence of 9.1 per 100,000 person-years and with poor prognosis due to high acute mortality and delayed cerebral injury [1, 2]. Pathophysiological mechanisms that underlie cerebral injury after SAH are complex and largely unresolved. Numerous animal studies, involving different experimental models, have been performed to elucidate pathophysiological processes after SAH. A frequently applied model that closely resembles the clinical pathology, involves perforation of the bifurcation of the internal carotid artery into the middle cerebral artery and anterior cerebral artery with an endovascular filament [3]. The arterial rupture leads to immediate extravasation of intracranial blood and acute elevation of intracranial pressure, resulting in significant reduction in cerebral perfusion within the first minutes [3–6]. In the following hours, intracranial pressure largely recovers, and perfusion is partially restored [6]. Nevertheless, cerebral blood flow (CBF) remains moderately lowered up to at least 6 h after the insult, which has been linked to persistent vessel narrowing [6]. For many years, vasospasm has been considered the primary cause of delayed ischemic injury after SAH; however, this concept is under debate, and other pathophysiological causes have also been suggested [7].

Assessment of concurrent perfusion and tissue changes at later stages after SAH would give further insights into progression of secondary complications and could provide targets for therapeutic intervention. This may be accomplished with noninvasive imaging methods that allow combined measurement of cerebral injury and hemodynamics [8]. The goal of our study was to characterize brain perfusion status and lesion progression at subacute to chronic time points in the clinically relevant endovascular perforation-induced SAH model in rats, based on serial multiparametric MRI along with repeated behavioral testing.

Methods

Animals

The Animal Experiments Committee of the University Medical Center Utrecht and Utrecht University approved the experiments conducted for this research (in accordance with the Experiments on Animals Act).

Male Wistar rats (320–350 g; Harlan, Horst, The Netherlands) were used ($n = 30$). Most animals were part of a drug treatment study in which animals received subcutaneous injection of either 0.022 mg/kg interferon-β ($n = 16$) or vehicle ($n = 14$) [9]. That study revealed no differences in lesion size, neurological status and mortality rate between treatment groups, and therefore, data were pooled. The current study reports original data on diffusion-weighted MRI, perfusion MRI and regional blood-brain barrier leakage that were not part of the treatment study and have not been published previously.

Experimental SAH

Animals were anesthetized by mechanical ventilation with 2% isoflurane in a mixture of air/oxygen (2:1) through an endotracheal tube. Animals received an intramuscular injection of 5 mg/kg (10 mg/ml) gentamicin (Centrafarm, Etten-Leur, The Netherlands) to prevent postoperative infection. The core temperature was maintained at 37.5°C using a temperature-controlled heating pad.

SAH was induced by intracranial endovascular perforation, for which a sharpened 4.0 prolene suture was transiently advanced into the right internal carotid artery to perforate it at the anterior cerebral artery and middle cerebral artery bifurcation [3, 10]. After surgery, animals received a subcutaneous injection of 0.03 mg/kg (0.03 mg/ml) buprenorphine (Reckitt and Colman, Kingston-upon-Hill, UK) for pain relief and a subcutaneous injection of 5 ml Ringer's lactate (Baxter, Utrecht, The Netherlands) in case of excessive weight loss.

Behavioral Assessment

Neurological deficits were measured before SAH (day –1, baseline score) and at days 1, 2, 3 and 7 after SAH, with a modified version of a battery of behavioral tests, described by Sugawara et al. [11]. Animals were scored on spontaneous activity (score 0–3), activity of extremities (score 0–3), forepaw outstretching (score 0–3), climbing reflex (score 1–3) and a forepaw placing response to the vibrissae touching the table side (score 1–3). The maximum score was 15 (absence of deficits).

Magnetic Resonance Imaging

MRI experiments were conducted at days 2 and 7 after SAH on an Agilent (Palo Alto, Calif., USA) 4.7-tesla horizontal bore MR system, with use of a 9-cm Helmholtz volume coil and an inductively coupled 2.5-cm surface coil.

Anesthesia was maintained in the same manner as described above. The core temperature was maintained at 37.5°C. Blood oxygenation, heart rate and expired CO_2 were continuously monitored and kept within physiological range.

For lesion detection, we applied diffusion-weighted MRI [spin echo eight-shot echo planar imaging; repetition time (TR) = 3,000 ms; echo time (TE) = 38.5 ms; b = 0 and 1,428 s/mm^2; 6 diffusion-weighting directions; field-of-view (FOV) = 32 × 32 × 19 mm^3; matrix size = 128 × 128 × 19; number of acquisitions (NA) = 2] and T2-weighted MRI (multiple spin echo; TR = 3,600 ms; TE = 15–180 ms; FOV = 32 × 32 × 19 mm^3; matrix size = 256 × 128 × 19; NA = 8). Diffusion- and T2-weighted MRI data were monoexponentially fitted to calculate maps of apparent diffusion coefficient (ADC) and T2, respectively.

For perfusion imaging, we conducted dynamic susceptibility contrast-enhanced MRI [gradient-echo echo planar imaging; TR = 330 ms; TE = 25 ms; flip angle = 35°; FOV = 32 × 32 × 9 mm^3; matrix size = 64 × 64 × 5 (1-mm interslice gap); NA = 1; number of repetitions = 400], in combination with an intravenous injection of 0.35 mmol/kg gadobutrol (Gadovist®, Schering, Kenilworth, N.J., USA). Maps of the hemodynamic parameters, cerebral blood volume (CBV), CBF index (CBF_i), and mean transit time (MTT) were calculated by block-circulant-based deconvolution of voxel-based tissue signal responses with an arterial input function measured in a contralateral region of the circle of Willis (2–3 voxels) [12].

Blood-brain barrier leakage was measured with T1-weighted MRI (gradient echo; TR = 160 ms; TE = 4 ms; FOV = 32 × 32 × 19 mm^3; matrix size = 256 × 128 × 19; NA = 8) acquired before and 22 min after contrast agent injection. Maps of contrast agent extravasation were calculated as relative contrast agent-induced change in T1-weighted MR signal intensity (rΔT1) on a voxel-by-voxel basis.

For all MRI-based maps, brain tissue was masked out and coregistered to a T2-weighted rat brain template. Lesioned tissue, characterized by signal hyperintensity, was manually outlined on multi-slice T2 maps. Rats without an ipsilateral lesion in the cortical MCA territory were excluded from further analysis (n = 2). Lesion outlines were combined to create a lesion incidence map. To select the primary lesion, we outlined tissue with a lesion incidence of ≥65%. This region of interest (ROI) was located in the ipsilateral somatosensory cortex (CXil). An ipsilateral region with a lesion incidence of 0%, which was located in the thalamus (THil), was also outlined. Homologous contralateral ROIs (i.e. CXcl and THcl) were automatically selected by mirroring across midline.

Statistics

Statistical analysis of time-dependent changes in tissue and perfusion status was done with repeated-measures ANOVA and post hoc Dunnett's testing. A Friedman test, with Dunn's post hoc analysis, was used to compare neurological scores over time. Comparison between values from animals that died and those that survived was done with Student's t test. Pearson's correlation testing was performed to evaluate relationships between different MRI-based parameters. Correlation analysis between MRI-based parameters and neurological scores was done using Spearman's rank correlation test. Values are presented as the mean ± standard deviation, unless otherwise mentioned. $p < 0.05$ was considered significant.

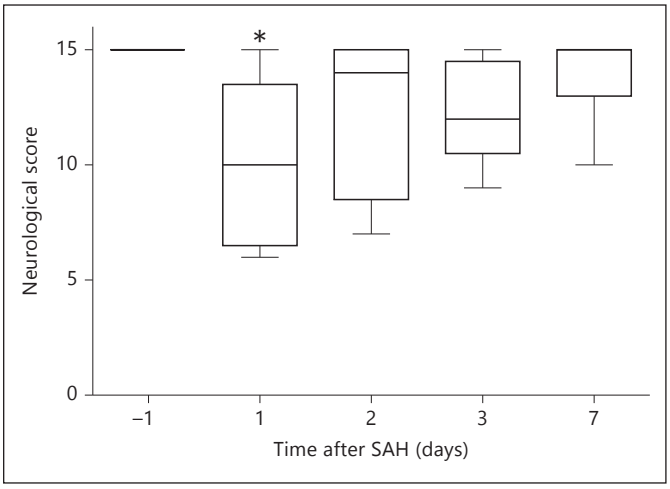

Fig. 1. Progression of neurological function after experimental SAH in rats. Box plot shows neurological score at baseline (day –1) and at days 1, 2, 3 and 7 after SAH in animals that completed the study protocol. * $p < 0.05$ versus baseline.

Results

Mortality and Neurological Deficits

Seventeen animals (57% of total) survived at least until the MRI session at 2 days after SAH, and 13 animals (43% of total) survived up to the final MRI session after 7 days.

The neurological score was significantly reduced at day 1 (9.8 ± 3.6) as compared to baseline (15.0 ± 0.0; $p < 0.05$) and (partially) recovered thereafter (13.7 ± 1.6 at day 7; fig. 1).

Brain Tissue and Perfusion Damage

Figure 2a shows representative maps of the T2, ADC, rΔT1 and CBF_i of a rat brain slice at 2 and 7 days after SAH. Clear T2 prolongation, ADC reduction, rΔT1 increase and CBF_i elevation were apparent at day 2 after SAH. After a week, CBF_i and rΔT1 were still elevated, while T2 prolongation was less obvious and ADC values were variable.

Lesion incidence maps (fig. 2b) demonstrated that tissue damage developed primarily in the ipsilateral sensorimotor cortex and caudate putamen. In most animals, the contralateral sensorimotor cortex was also affected. No tissue damage was observed in the ipsi- or contralateral thalamus. T2-based lesion volumes were 166 ± 139 and 73 ± 84 mm^3 at days 2 and 7, respectively, in animals that survived the entire protocol. Animals that died after the first MRI session at day 2 had significantly larger lesion volumes (374 ± 79 mm^3; $p < 0.05$). Neurological out-

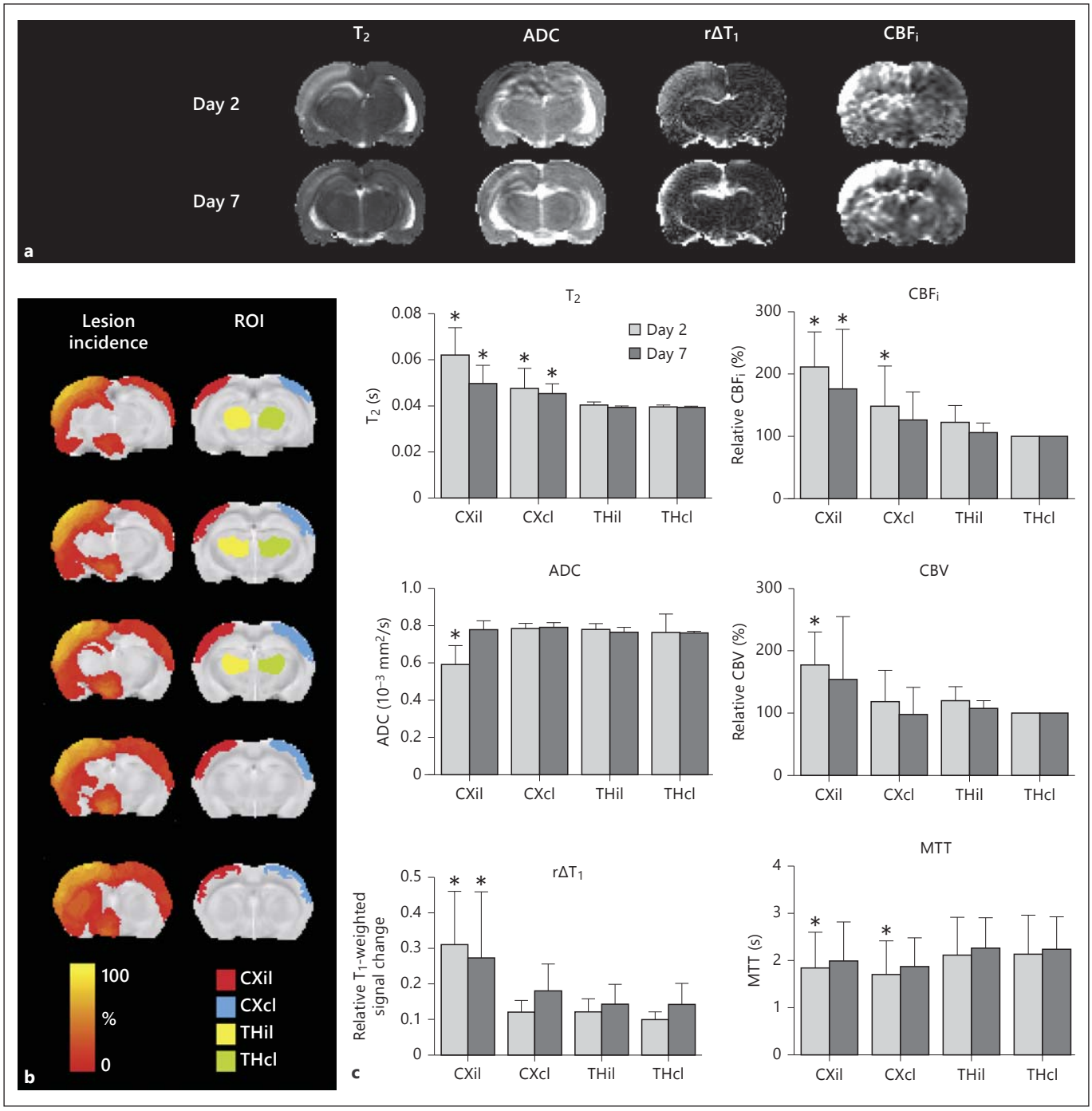

Color version available online

Fig. 2. Progression of tissue and perfusion changes after experimental SAH in rats. **a** Typical examples of parametric maps of T2, ADC, rΔT1 and CBF_i in a coronal rat brain slice at 2 and 7 days after SAH. **b** Coronal slices from a T2-weighted rat brain template overlaid by lesion incidence map (0–100%) and ROIs, i.e. CXil (red), CXcl (blue), THil (yellow) and THcl (green). The colors refer to the online version of the figure. **c** MRI parameter values (mean ± SD) in CXil, CXcl, THil and THcl at days 2 and 7 after SAH. CBF_i and CBV are expressed as percentage of values in THcl. * $p < 0.05$ versus THcl.

Cerebrovasc Dis 2013;36:167–172
DOI: 10.1159/000352048

come correlated negatively with brain lesion volume at day 7 ($r = -0.80$; $p < 0.05$).

Values of MRI-based tissue and perfusion parameters in the different ROIs (displayed in fig. 2b) at days 2 and 7 after SAH are shown in figure 2c. T2 prolongation was significant at both time points in CXil and CXcl (there were no significant differences between treatment groups; data not shown). A significant reduction in ADC was observed in CXil at day 2, while a mixture of cortical areas with reduced and elevated ADC values at day 7 resulted in a pseudonormal overall ADC. Extravasation of contrast agent was evident from significant rΔT1 in CXil at days 2 and 7. ADC and rΔT1 were not significantly altered in CXcl. In THil and THcl, T2, ADC and rΔT1 values remained unchanged at both time points.

At day 2, both CBF_i and CBV were significantly elevated in CXil, while MTT was significantly shortened (fig. 2c). Significant CBF_i increase and MTT decrease at day 2 were also detected in CXcl. CBF_i in CXil remained significantly increased at day 7. There were no significant differences between treatment groups (e.g., relative CBF_i, expressed as percentage of level in THcl, in CXil was 201 ± 37 and 226 ± 76% at day 2 and 166 ± 73 and 189 ± 126% at day 7 in interferon-β- and vehicle-treated animals, respectively). Animals that died between 2 and 7 days after SAH had significantly higher relative CBF_i in THil (154 ± 9%) and relative CBV in THil (144 ± 11%) and CXil (241 ± 115%) at day 2, as compared to surviving animals (relative CBF_i in THil: 114 ± 24%; relative CBV in THil: 113 ± 20%; relative CBV in CXil: 160 ± 46%; $p < 0.05$).

Correlation analysis of tissue and perfusion parameters for all ROIs revealed that an increase in CBF_i correlated significantly with increased T2 and rΔT1 values at both time points (table 1). Positive correlations were also found for subacute CBF_i at day 2 versus chronic T2 and rΔT1 at day 7. Significant negative and positive correlations were found between CBF_i and ADC at days 2 and 7, respectively.

Table 1. Correlations between perfusion and tissue indices at days 2 and 7 after experimental SAH in rats

CBF_i	Day 2			Day 7		
	T2	ADC	rΔT1	T2	ADC	rΔT1
Day 2						
r	0.78	–0.75	0.87	0.66	0.26	0.53
p	<0.05	<0.05	<0.05	<0.05	0.09	<0.05
Day 7						
r				0.85	0.63	0.74
p				<0.05	<0.05	<0.05

Discussion

In this study, we applied serial MRI to characterize and correlate patterns of tissue damage and perfusion changes at subacute and chronic stages after experimental SAH induced by rupture of the internal carotid artery at its intracranial bifurcation in rats. In line with earlier studies that employed this endovascular perforation model [3–5], we observed high acute mortality (43%) that matches mortality rates of about 40% after clinical aneurysmal SAH [13, 14]. Previous studies with this model have primarily focused on the first 24 h after SAH [5]. The current longitudinal imaging study demonstrates that surviving animals suffer from ipsi- and contralateral brain lesions with subacute cytotoxic edema (i.e. ADC reduction), blood-brain barrier disruption (i.e. contrast agent extravasation) and vasogenic edema (i.e. T2 prolongation) that last during the chronic phase. Subacute mortality was associated with extensive lesion size and raised ipsilateral perfusion levels. Lesioned areas exhibited blood-brain barrier leakage; however, the most striking finding was that hyperperfusion occurred in the area of brain injury at subacute as well as chronic stages after SAH. The elevated CBF_i correlated significantly with edema and blood-brain barrier permeability.

Despite the occurrence of initial ischemia, our MRI data show that significantly elevated CBF and CBV in lesioned tissue are evident at later stages. While pial vasoconstrictions – e.g., as a consequence of direct contact to subarachnoid blood – may persist [15], the observed rise in intraparenchymal blood flow seems to refute enduring local hypoperfusion as cause of delayed ischemic injury. Although ADC and T2 (partially) normalized, lesioned ipsilateral cortical regions displayed increased perfusion together with blood-brain barrier injury and edema up to day 7. Furthermore, subacutely elevated CBF_i was predictive of chronic tissue edema, which could indicate ischemia-reperfusion injury, i.e. exacerbation of tissue damage following restoration of blood flow in previously ischemic areas [16]. This post-SAH hyperperfusion may be reflective of a dysfunctional vasculature with impaired autoregulation and/or endothelial disruption. Our findings of subacute blood-brain barrier leakage – persisting up to day 7 – which colocalized with the area with elevated CBF, suggest that post-SAH hyperperfusion may have contributed to the initiation or exacerbation of blood-

brain barrier disruption and subsequent vasogenic edema. On the other hand, we cannot exclude that post-SAH hyperperfusion may also have contributed to the prevention or reduction of delayed cerebral ischemia.

Although chronic hyperperfusion has not been previously described for the current rat SAH model, it is not a model-specific phenomenon, as posthemorrhagic hyperemia after 2 days has previously been reported in a primate study [17]. Moreover, hyperperfusion [18, 19] as well as postischemic flow recovery [20] have also been observed in aneurysmal SAH patients in chronic phases.

In conclusion, our imaging study suggests that SAH-induced brain injury at later stages is associated with progressive changes in tissue perfusion. Moreover, hyperperfusion in brain lesions may seriously worsen the outcome and could explain, for instance, why triple-H therapy – the combination of induced hypertension, hypervolemia and hemodilution – for delayed cerebral ischemia in SAH patients is not always successful and can even be detrimental [21]. Multiparametric MRI may significantly aid in diagnosing the brain status after SAH; however, further research is required to establish if and to what extent elevated CBF after SAH contributes to progression of cerebral injury or reflects a pathophysiological epiphenomenon.

Acknowledgements

This research has received funding from the Netherlands Heart Foundation (2005B156), the Netherlands Brain Foundation (15F07(2).08) and the European Union's Seventh Framework Programme (FP7/2007-2013) under grant agreements No. 201024 and No. 202213 (European Stroke Network).

References

1 Van Gijn J, Kerr RS, Rinkel GJ: Subarachnoid haemorrhage. Lancet 2007;369:306–318.
2 Steiner T, Juvela S, Unterberg A, Jung C, Forsting M, Rinkel G: European stroke organization guidelines for the management of intracranial aneurysms and subarachnoid haemorrhage. Cerebrovasc Dis 2013;35:93–112.
3 Bederson JB, Germano IM, Guarino L: Cortical blood flow and cerebral perfusion pressure in a new noncraniotomy model of subarachnoid hemorrhage in the rat. Stroke 1995;26:1086–1091.
4 Prunell GF, Mathiesen T, Diemer NH, Svendgaard NA: Experimental subarachnoid hemorrhage: subarachnoid blood volume, mortality rate, neuronal death, cerebral blood flow, and perfusion pressure in three different rat models. Neurosurgery 2003;52:165–175.
5 Lee JY, Sagher O, Keep R, Hua Y, Xi G: Comparison of experimental rat models of early brain injury after subarachnoid hemorrhage. Neurosurgery 2009;65:331–343.
6 Westermaier T, Jauss A, Eriskat J, Kunze E, Roosen K: Time-course of cerebral perfusion and tissue oxygenation in the first 6 h after experimental subarachnoid hemorrhage in rats. J Cereb Blood Flow Metab 2009;29:771–779.
7 Pluta RM, Hansen-Schwartz J, Dreier J, Vajkoczy P, Macdonald RL, Nishizawa S, Kasuya H, Wellman G, Keller E, Zauner A, Dorsch N, Clark J, Ono S, Kiris T, Leroux P, Zhang JH: Cerebral vasospasm following subarachnoid hemorrhage: time for a new world of thought. Neurol Res 2009;31:151–158.
8 Dijkhuizen RM, Nicolay K: Magnetic resonance imaging in experimental models of brain disorders. J Cereb Blood Flow Metab 2003;23:1383–1402.
9 Tiebosch IA, Dijkhuizen RM, Cobelens PM, Bouts MJ, Zwartbol R, Van der Meide PH, Van den Bergh WM: Effect of interferon-beta on neuroinflammation, brain injury and neurological outcome after experimental subarachnoid hemorrhage. Neurocrit Care 2013;18:96–105.
10 Van den Bergh WM, Zuur JK, Kamerling NA, van Asseldonk JT, Rinkel GJ, Tulleken CA, Nicolay K: Role of magnesium in the reduction of ischemic depolarization and lesion volume after experimental subarachnoid hemorrhage. J Neurosurg 2002;97:416–422.
11 Sugawara T, Ayer R, Jadhav V, Zhang JH: A new grading system evaluating bleeding scale in filament perforation subarachnoid hemorrhage rat model. J Neurosci Methods 2008;167:327–334.
12 Wu O, Ostergaard L, Weisskoff RM, Benner T, Rosen BR, Sorensen AG: Tracer arrival timing-insensitive technique for estimating flow in MR perfusion-weighted imaging using singular value decomposition with a block-circulant deconvolution matrix. Magn Reson Med 2003;50:164–174.
13 Pakarinen S: Incidence, aetiology, and prognosis of primary subarachnoid haemorrhage. A study based on 589 cases diagnosed in a defined urban population during a defined period. Acta Neurol Scand 1967;43(suppl 29):1–28.
14 Nieuwkamp DJ, Setz LE, Algra A, Linn FH, de Rooij NK, Rinkel GJ: Changes in case fatality of aneurysmal subarachnoid haemorrhage over time, according to age, sex, and region: a meta-analysis. Lancet Neurol 2009;8:635–642.
15 Friedrich B, Müller F, Feiler S, Schöller K, Plesnila N: Experimental subarachnoid hemorrhage causes early and long-lasting microarterial constriction and microthrombosis: an in-vivo microscopy study. J Cereb Blood Flow Metab 2012;32:447–455.
16 Girn HR, Ahilathirunayagam S, Mavor AI, Homer-Vanniasinkam S: Reperfusion syndrome: cellular mechanisms of microvascular dysfunction and potential therapeutic strategies. Vasc Endovascular Surg 2007;41:277–293.
17 Jakubowski J, Bell BA, Symon L, Zawirski MB, Francis DM: A primate model of subarachnoid hemorrhage: change in regional cerebral blood flow, autoregulation carbon dioxide reactivity, and central conduction time. Stroke 1982;13:601–611.
18 Rothoerl RD, Woertgen C, Brawanski A: Hyperemia following aneurysmal subarachnoid hemorrhage: incidence, diagnosis, clinical features, and outcome. Intensive Care Med 2004;30:1298–1302.
19 Chieregato A, Tagliaferri F, Tanfani A, Cocciolo F, Benedettini W, Compagnone C, Ravaldini M, Pascarella R, Battaglia R, Frattarelli M, Targa L, Fainardi E: Cerebral blood flow in mean cerebral artery low density areas is not always ischemic in patients with aneurysmal subarachnoid hemorrhage – relationship with neurological outcome. Acta Neurochir Suppl 2005;95:153–158.
20 Dankbaar JW, de Rooij NK, Smit EJ, Velthuis BK, Frijns CJ, Rinkel GJ, van der Schaaf IC: Changes in cerebral perfusion around the time of delayed cerebral ischemia in subarachnoid hemorrhage patients. Cerebrovasc Dis 2011;32:133–140.
21 Lee KH, Lukovits T, Friedman JA: 'Triple-H' therapy for cerebral vasospasm following subarachnoid hemorrhage. Neurocrit Care 2006;4:68–76.